applied sciences

MDPI

Article

The Limitation of Unproductive Binding of Cellulases to Lignin by Ozone Pretreatment

Congfei Zhang, Lihong Zhao *, Weiying Li, Junli Ren, Hongyuan Wang and Beihai He

State Key Laboratory of Pulp and Paper Engineering, South China University of Technology, Guangzhou 510641, China; 202120129365@mail.scut.edu.cn (C.Z.); feweiyingli@scut.edu.cn (W.L.); renjunli@scut.edu.cn (J.R.); 201920126978@mail.scut.edu.cn (H.W.); ppebhhe@scut.edu.cn (B.H.)

* Correspondence: zhaolh@scut.edu.cn

Abstract: The limitation of enzymatic saccharification of lignocellulose is attributed to the nonproductive adsorption between lignin and cellulase. This study aims to investigate the effects of ozone pretreatment on the physical structure and chemical properties of milled wood lignin (MWL). The objective is to reduce the non-productive adsorption of cellulase on lignin. The structure–activity relationship between the physical structure of MWL and the occurrence of nonproductive adsorption was analysed using two-dimensional heteronuclear single quantum coherence–nuclear magnetic resonance (HSQC-NMR) and phosphorus-31 nuclear magnetic resonance spectrum (^{31}P-NMR), etc. The results indicate that ozone pretreatment resulted in a decrease in the phenolic hydroxyl content and S/G ratio, an increase in the carboxyl content, and a negative zeta potential of MWL. The maximum adsorption capacity decreased from 25.77 mg/g to 10.09 mg/g, the Langmuir constant decreased from 13.86 mL/mg to 10.11 mL/mg, and the binding strength decreased from 357.14 mL/g to 102.04 mL/g, as determined by Langmuir isothermal adsorption. This suggests that ozone pretreatment resulted in a reduction in the hydrophobicity of lignin and a weakening of the electrostatic attraction between lignin and cellulase, thereby effectively reducing the non-productive adsorption of cellulase on lignin. This study provides an environmentally friendly pretreatment technique and comprehensively analyses the structural changes of ozone-treated MWL. These findings contribute to a deeper understanding of the interaction between lignin and cellulase.

Keywords: non-productive adsorption; ozone pretreatment; milled wood lignin

Citation: Zhang, C.; Zhao, L.; Li, W.; Ren, J.; Wang, H.; He, B. The Limitation of Unproductive Binding of Cellulases to Lignin by Ozone Pretreatment. *Appl. Sci.* **2024**, *14*, 2318. https://doi.org/10.3390/app14062318

Academic Editor: Alejandro Rodríguez Pascual

Received: 2 January 2024
Revised: 15 February 2024
Accepted: 19 February 2024
Published: 9 March 2024

1. Introduction

The depletion of non-renewable resources and the ecological crisis have made lignocellulose an alternative biomass resource to petroleum-based feedstocks [1]. For instance, enzymatic hydrolysis in biomass refining facilitates the conversion of cellulose and hemicellulose into monosaccharides, which can be further converted into chemicals and biofuels such as ethanol [2], lactic acid [3], butanol [4], and levulinic acid [5].

However, the utilization of lignocellulose is impeded by its structural complexity, resulting in challenges in lignin solubilisation and the irreversible non-productive adsorption of cellulase onto residual lignin within cellulose fibres. This adsorption is facilitated by hydrophobicity, electrostatics, and hydrogen bonding interactions during the hydrolysis process [6]. The prevailing consensus is that hydrophobic interactions primarily contribute to the non-productive adsorption of cellulase onto lignin. The cellulase enzyme contains hydrophobic groups, such as aromatic amino acids, which possess binding sites for hydrophobic interactions. These hydrophobic groups, including phenol hydroxyl and methoxy, exhibit a preference for recognizing the hydrophobic groups present on the surface of lignin. Consequently, during the process of enzymatic hydrolysis, cellulase tends to adsorb preferentially to lignin [7]. The ionization and association of distinct chemical groups in both lignin and cellulase can result in the development of net charges on the

surfaces of both the lignin and the enzyme. This charge distribution may potentially lead to an attractive force between the lignin and the enzyme [8,9]. Furthermore, the presence of hydroxyl groups in both lignin and cellulase may also contribute to this adsorption by facilitating hydrogen bond formation [10]. The reducing end of the cellulose chain can engage in hydrogen bonding with the phenolic hydroxyl group in the amino acid residue of cellulase Cel7A at the 10 binding sites. This interaction facilitates the entry of cellulose into the catalytic channel of the enzyme, thereby enhancing its effective degradation. Conversely, lignin's phenolic hydroxyl group is also capable of forming hydrogen bonds with cellulase's hydroxyl group; however, this interaction hinders enzyme hydrolysis [11]. It has been observed that during enzymatic hydrolysis, cellulase can irreversibly and non-productively adsorb onto lignin, resulting in some of the adsorption sites within the cellulase catalytic channel becoming occupied by lignin.

Due to the compact structure and intricate chemical composition of lignocellulosic biomass, it is common practice to employ acids, alkalis, etc., to dissolve lignin [12]. Ozone is known for its significant chemical reactivity due to its high oxidation potential of 2.07 V [13]. Barrera-Martínez et al., observed that the alkali lignin and sugarcane bagasse were pretreated by an ozonification process, leading to the double bonds (C=C) on lignin of the lateral chains being oxidized to alcohols, esters, or acid groups. Additionally, the lignin present in bagasse was oxidized from the beginning, which facilitated enhanced lignin removal and enzymatic hydrolysis [14]. The benzene ring present in both phenolic and non-phenolic structures of lignin engages in ring-opening reactions with ozone molecules, leading to the disruption of the aromatic ring. Additionally, carbon–carbon double bonds, ether bonds, hydroxyl groups, and unsaturated double bonds within the molecular side chains of lignin can undergo oxidation, resulting in the formation of hydrophilic groups such as carboxyl, carbonyl, and aldehyde. Rosen et al., pretreated oat straw with ozone and dilute sulfuric acid at low temperatures, and it was observed that ozone exhibited a preference for attacking and selectively degrading phenolic lignin, resulting in the formation of hydroxyl radicals (•OH) in an aqueous solution. This process facilitated enzymatic hydrolysis and saccharification, particularly the conversion of xylose [15]. Our previous study found that ozone pretreatment reduced the hydrophobicity and enhanced the negative surface charge of alkali lignin, thereby facilitating the enzymatic hydrolysis of cellulose [16]. However, the effect of changes in the phenolic hydroxyl content of ozone-pretreated lignin on the adsorption of cellulase has not been investigated in our previous studies. Despite extensive research conducted on the removal of lignin using ozone and promoting the enzymatic hydrolysis of cellulose, there is a lack of studies elucidating the underlying mechanisms that enhance enzymatic hydrolysis efficiency by examining factors influencing non-productive adsorption between MWL and cellulase resulting from ozone treatment.

The aim of this study was to examine the impact of ozone pretreatment on the physical structure and chemical properties of MWL, as well as its effect on the non-productive adsorption of cellulase. This was accomplished by utilizing ^{31}P-NMR, HSQC-NMR, FTIR, and GPC to elucidate the structural characteristics of MWL. Moreover, Langmuir adsorption isotherms, hydrophobicity, and zeta potentials were employed to characterize the adsorption of cellulase onto lignin. This will enhance our understanding of the interaction between lignin and cellulase and ultimately improve biotechnological processes.

2. Materials and Methods

2.1. Materials

The MWL extracted from bamboo fibre (*Neosinocalamus affinis*) was provided by Xingu Environmental Co., Ltd. (Anhui, China). It was then purified by dissolving in an organic solvent (dioxane:water = 96:4) and extracted from light-avoiding conditions for 48 h to precipitate until the supernatant was clarified. Finally, the MWL was washed and dried. The cellulase (Cellulast 1.5 L) and the filter paper with enzyme activity of 81 FPU/mL were purchased from Sigma-Aldrich (St. Louis, MO, USA).

Chemicals

Pyridine, acetic anhydride, tetrahydrofuran, and H_2SO_4 were purchased from Tianjin Fuyu Chemical Co. (Tianjin, China). Rose Bengal Dye and citric acid monohydrate were purchased from Shanghai Yuanye Biotechnology Co. (Shanghai, China). Deuterated dimethyl sulfoxide (DMSO-d6), deuterated pyridine, deuterated chloroform, cyclohexanol, chromium acetylacetonate, and 2-chloro-4,4,5,5-tetramethyl-1,3,2-dioxaphospholane (TMDP) were purchased from Shanghai Macklin Biochemistry Technology Co. (Shanghai, China).

2.2. Ozone Pretreatment

Firstly, 5 g of MWL was placed in a homemade reaction kettle, and deionized water was added to maintain a solution concentration of 2 w/v%. The solution pH was adjusted to 2 using H_2SO_4. Then, the MWL was treated with ozone at a concentration of 85 mg/L and a flow rate of 3 L/min for 60 min and 120 min at room temperature. After ozonation, the samples were washed with deionized water and vacuum filtered to eliminate possible inhibitors; finally, the product was vacuum dried at 40 °C. The yields recovered from OL 60 and OL 120 after ozone pretreatment were 99.30% and 98.96%. The untreated lignin and lignin obtained by ozone treatment at 60 min and 120 min are named MWL, OL 60, and OL 120, respectively.

2.3. Analysis Procedures

2.3.1. Fourier-Transform Infrared Spectrum (FTIR) Analysis

The potassium bromide (KBr) tablet method was used for the FTIR analysis. The samples were crushed into powder and sieved through a 200 mesh sieve, followed by drying in an oven at 105 °C for 6 h. The dried samples were then mixed with KBr at a mass ratio of 1:100 under infrared irradiation and scanned 64 times over a wavelength range of 4000–500 cm^{-1} with a resolution of 4 cm^{-1}. Each spectrum was analysed by taking a normalization of a baseline and using the height ratio of the significant functional groups.

2.3.2. Phosphorus-31 Nuclear Magnetic Resonance Spectrum (^{31}P-NMR) Analysis

Quantitative ^{31}P-NMR analysis was performed on 500M NMR to determine the amounts and distribution of various hydroxyl groups in lignin. ^{31}P-NMR spectra were acquired after phosphitylation of lignin with TMDP (2-chloro-4,4,5,5-tetramethyl-1,3,2-dioxaphospholane) [17–19]. The parameters for ^{31}P-NMR spectra were as follows: a 90° pulse angle, 0.4 s acquisition time, 5 s relaxation delay, and 256 scans at 25 ± 5 °C.

2.3.3. Two-Dimensional Heteronuclear Single Quantum Coherence–Nuclear Magnetic Resonance (HSQC-NMR) Spectral Analysis

A total of 100 mg of lignin sample was added to 100 mL of DMSO-d6 and dissolved using a vortex oscillator. Subsequently, the resulting DMSO-d6 solution was filtered through a 0.22 μm filter to ensure its transparency and uniformity. The filtered solution was then transferred into the nuclear magnetic tube for HSQC-NMR analysis. The HSQC-NMR analysis was conducted using a 500 MHz nuclear magnetic resonance instrument. The experimental parameters included the utilization of the pulse program HSQCGP, a relaxation time of 1.5 s, an accumulation of 64 times, and a number of acquisition points: 1TD = 2500, 2TD = 526, number of scans (NS) = 75, and total test time = 10 h. The chemical shift of DMSO-d6 (δ_C 39.53 ppm, δ_H 2.51 ppm) was used as a calibration standard. The acquired data of NMR were processed using Top Spin 3.6.4 software.

2.3.4. Rose Bengal Dye Analysis

The surface hydrophobicity of lignin was determined by the Rose Bengal dye method [20]: 0.02 g, 0.04 g, 0.06 g, 0.08 g, and 0.10 g of lignin samples were weighed, and each sample was dissolved in 10 mL of Rose Bengal red citric acid–sodium citrate buffer solution with a concentration of 40 mg/L. The solutions were incubated at 50 °C and 150 rpm for 2 h. Following incubation, the supernatant was utilized to quantify the absorbance at 543 nm using a UV spectrophotometer. The absorbance value serves as an indicator of the quantity

of unbound Rose Bengal dye present in the reaction system subsequent to incubation (based on the standard curve of Rose Bengal concentration–absorbance). The partition coefficient (PQ) is defined as the ratio of the adsorbed-dye quantity to the unbound-dye quantity. The hydrophobicity of lignin (ranging from 2–10 g/L) was graphed against PQ, and the slope of the fitted line represents the hydrophobicity of lignin.

2.3.5. Zeta Potential Analysis

A solution of citric acid–sodium citrate with a lignin concentration of 0.1 w/v% was prepared and subjected to oscillation at 180 rpm at a temperature of 50 °C in a water bath oscillator for a duration of 1 h. Following centrifugation at 6000 rpm for 5 min, the resulting supernatant was utilized for zeta potential analysis in order to characterize the charge present on the surface of the lignin. The zeta potential analysis was conducted using a Malvern (UK) zeta potential analyser (Malvern Instruments Ltd., Malvern, UK).

2.3.6. Gel Permeation Chromatography (GPC) Analysis

The GPC technique was used to determine the weight average molecular weight (Mw) and number average molecular weight (Mn) of the samples. In a centrifuge tube, 30 mg of lignin was dissolved in a mixture of 1.5 mL pyridine-acetic anhydride (volume ratio 1:2). To remove air, nitrogen was injected into the centrifuge tube, which was then placed in a dark environment for 72 h. [21]. Following the acetylation reaction, 20 mL of ether was gradually added to the centrifuge tube. The mixture was centrifuged at 8000 rpm for 5 min, and the resulting precipitated lignin was washed multiple times with ether to remove any residual pyridine on its surface. Subsequently, the lignin was dried in a vacuum drying oven at a temperature of 40 °C for a duration of 24 h for further use. A quantity of 3 mg of acetylated lignin was then weighed and dissolved in 3 mL of tetrahydrofuran. The resulting tetrahydrofuran solution was filtered using a 0.45 μm organic phase filter. Finally, the molecular weight was estimated by size exclusion separation on an Agilent 1200 HPLC system (Agilent Technologies, Inc., Santa Clara, CA, USA) equipped with Waters Styragel columns (HR5E and HR1; Waters Corporation, Milford, MA, USA). The mobile phase was THF (HPLC grade) with a flow rate of 0.6 mL/min, at 50 °C.

2.4. Lignin and Cellulase Langmuir-Adsorption Analysis

Cellulase adsorption experiments were performed following the previous methods to determine the concentration of free cellulase [16]. The amount of cellulase that had been adsorbed was calculated as the difference between the initial cellulase concentration and the concentration of free cellulase. Bovine serum albumin (BSA) was used as the protein standard sample, and the content of free cellulase was detected by the BCA kit method.

The Langmuir adsorption isotherm equations are shown in Equations (1) and (2) [22]:

$$1/\Gamma = 1/(K \cdot \Gamma_{max} \cdot C) + 1/\Gamma_{max} \quad (1)$$

$$R = \Gamma_{max} \cdot K \quad (2)$$

where Γ is the concentration of adsorbed cellulase (mg/g lignin); C is the free cellulase concentration (mg/mL); K is the Langmuir constant (mL/mg); Γ_{max} is the maximum adsorbed cellulase amount (mg/g lignin); and R is the binding strength (mL/g).

3. Results and Discussion

3.1. FTIR Determination

The FTIR analysis of lignin was performed to investigate the changes in chemical structure and functional groups of lignin molecules before and after ozone treatment (Figure 1). The calculation of the relative signal intensity for each group was performed by referring to the intensity in the 1426 cm^{-1} band, as shown in Table 1. No distinct shift in the positions of the absorption peaks of lignin before and after pretreatment was observed, indicating that the ozone pretreatment did not change the main molecular structure of

lignin. The characteristic absorption peaks at 1426, 1514, and 1606 cm^{-1} are ascribed to the aromatic ring skeleton of lignin, the signal peak at 1705 cm^{-1} is associated with the unconjugated carbonyl group (C=O), the peak at 2932 cm^{-1} is designated as C-H stretching vibration in methoxy (-OCH_3), the peaks at 1113 cm^{-1} represent the C-H deformation inside the aromatic ring on the syringyl aromatic ring [23], and the peak at 3451 cm^{-1} is attributed to the stretching vibration absorption of -OH including aliphatic and phenolic hydroxyl groups [24–26]. The infrared spectra showed different signal intensities for the three MWL samples, indicating that the monomer units of MWL were altered after ozone treatment. The intensity of the hydroxyl absorption peak increased with the increase in ozone pretreatment time. This could be attributed to the ozone oxidation process, which breaks ether bonds and results in the formation of additional hydroxyl groups. The small reduction in the intensity of the methoxy absorption peak may be due to the demethylation reaction of the lignin molecular chain induced by ozone, which may lead to a weakened hydrophobicity of lignin. This result presented in FTIR spectrograms needs to be further demonstrated by ^{31}P-NMR and HSQC-NMR analysis.

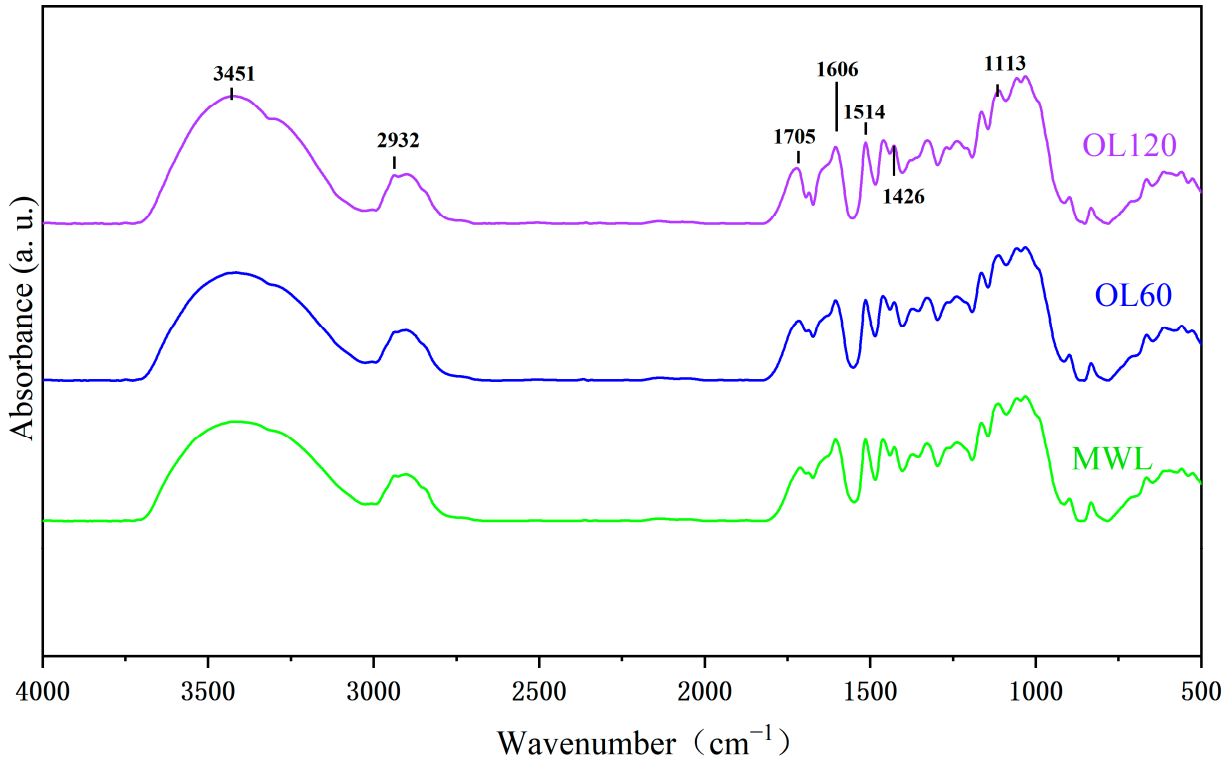

Figure 1. The FTIR spectra of lignin before and after ozone pretreatment.

Table 1. The proportion of typical lignin absorption-peak intensity based on the 1426 cm^{-1} band.

Assignment	Wavenumber cm^{-1}	MWL	OL60	OL120
Hydroxyl group	3451	1.08	1.15	1.18
C-H stretching	2932	1.03	1.01	0.98
Carbonyl group	1705	1.06	1.11	1.12
Aromatic ring	1606	0.97	1.02	1.05
Aromatic ring	1514	0.98	0.97	0.98
Aromatic ring	1426	1.00	1.00	1.00
Aromatic C-H deformation in syringyl	1113	0.81	0.77	0.76

3.2. ^{31}P-NMR Determination

Phosphorus nuclear magnetic resonance spectroscopy (^{31}P-NMR) was employed to quantitatively analyse the presence of various hydroxyl and carboxyl groups in lignin (Figure 2). This was achieved by replacing the unstable hydrogen atoms with a phosphorylation reagent (TMDP), to generate lignin-TMDP derivatives. Signal peaks corresponding to different types of hydroxyl groups were observed at specific regions, including aliphatic hydroxyl (149.1–146.3 ppm), condensed phenolic hydroxyl (144.5–143.4 ppm), (142.0–141.3 ppm), syringyl phenolic hydroxyl (143.5–142.1 ppm), guaiacyl phenolic hydroxyl (140.1–138.8 ppm), p-hydroxyphenyl phenolic hydroxyl (138.3–137.1 ppm), and carboxyl (135.3–134.0 ppm) [27,28]. The quantitative calculations of the NMR phosphorus spectra for each lignin sample are shown in Table 2. Following ozone pretreatment, the total phenolic hydroxyl content in MWL exhibited a significant decrease, while the carboxyl content showed an increase. This can be attributed to the oxidation of ozone molecules leading to the conversion of hydroxyl groups on the benzene ring into carboxyl or carbonyl groups [29,30]; this conclusion is consistent with the results of our previous study [16]. Previous literature suggested that the phenolic hydroxyl groups present in lignin can form hydrogen bonds with hydroxyl groups in cellulase. Additionally, lignin has the ability to bind with nucleophilic sites in the molecular structure of cellulase, resulting in the formation of quinone methylation intermediates, which adversely affect enzymatic digestion [10]. Consequently, during the process of enzymatic hydrolysis, lignin may undergo non-productive adsorption with cellulase through the formation of hydrogen bonds. This can lead to the occupation of some of the adsorption sites within the cellulase catalytic channel by lignin, ultimately hindering the enzymatic hydrolysis of cellulose. Therefore, the decrease in phenolic hydroxyl content in MWL is advantageous for mitigating ineffective adsorption between lignin and cellulase, as the presence of phenolic hydroxyl groups positively correlates with the formation of hydrogen bonds between cellulase and lignin [31]. Consequently, the reduction in phenolic hydroxyl content also signifies a decrease in the strength of the hydrogen-bonding interaction between the two entities. Conversely, the augmentation of carboxyl content in MWL not only amplifies the hydrophilicity of lignin but also augments the negative charge density on the surface of lignin, thereby enhancing its electrostatic repulsion towards cellulase.

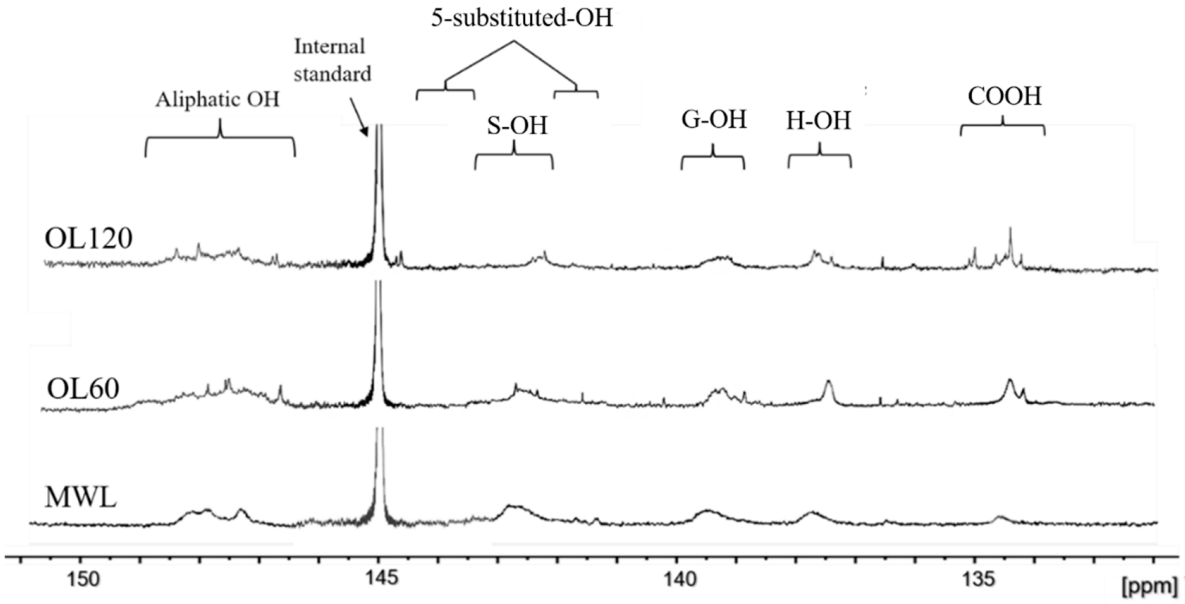

Figure 2. ^{31}P-NMR spectra of MWL samples.

Table 2. Content of the various hydroxyl groups of lignin samples quantified by ^{31}P-NMR.

Lignin Structure	Lignin Samples (mmol/g)		
	MWL	OL60	OL120
Aliphatic hydroxyl	2.13	1.88	1.75
5-substituted-OH	1.08	0.88	0.79
G-OH	0.49	0.43	0.44
H-OH	0.69	0.66	0.65
Total phenol hydroxyl	2.26	1.97	1.88
COOH	0.21	0.30	0.47

3.3. HSQC-NMR Determination

The determination of C-H bonds in the lignin structure was conducted using HSQC-NMR for qualitative and semi-quantitative analysis of the fundamental structural units and primary connecting bonds of lignin. Following a method described in the literature, the guaiacyl, syringyl, p-hydroxyphenyl structural units, and major linkage bonds such as aryl ether bonds in lignin were analysed semi-quantitatively [32]. The HSQC-NMR spectra of lignin encompassed the benzene ring region (100–150/6.0–8.0 ppm) and the side chain region (50–90/2.5–6.0 ppm) (Figure 3). Within the side chain region, the signal peaks corresponding to the Cα-Hα and Cβ-Hβ bonds in the aryl ether bond (β-O-4) were observed at 71.7/4.83 ppm and 86.3/4.04 ppm, respectively. The signal peaks attributed to the resinol (β-β) were detected at 84.9/4.65 ppm and 53.5/3.06 ppm for the Cα-Hα and Cβ-Hβ bonds, respectively. Additionally, the signal peaks associated with β-5 were observed at 86.9/5.46 ppm for the Cα-Hα bond and 53.8/3.51 ppm for the Cβ-Hβ bond. Lastly, the signal corresponding to methoxy was detected at 55.5/3.7 ppm [26]. The findings of the semi-quantitative analysis are shown in Table 3. The aryl ether bond, being the primary linkage bond in lignin, experienced a slight increase in the number of bonds after ozone pretreatment of MWL. In the region of the benzene ring, the syringyl unit (S) exhibited a signal at 104.5/6.67 ppm, while the oxidized syringyl unit (S′) displayed a signal at 101.4/7.22 ppm. The signals at 111.0/6.98 ppm, 115.6/6.71 ppm, and 119.5/6.78 ppm were assigned to the C2-H2, C5-H5, and C6-H6 bonds, respectively, in the guaiacyl units (G2, G5, G6). The C2,6-H2,6 in p-hydroxyphenyl units (H) were characterized by signal peaks at 128.0/7.18 ppm [32,33]. Additionally, the signals corresponding to p-coumaric acid (p-CA) C2/6-H2/6, Cα-Hα, and Cβ-Hβ were detected at 130.6/7.48 ppm, 145.1/7.45 ppm, and 114.2/6.28 ppm, respectively. Similarly, the signals for ferulate (FA) Cα-Hα and Cβ-Hβ were observed at 145.2/7.26 ppm and 114.2/6.14 ppm, respectively [34]. Following ozone pretreatment, the relative content of S-type structural units was lower than that in MWL, while the relative content of other structural units increased slightly. On one hand, the observed phenomenon can be attributed to the elimination of methoxy groups from S-type phenyl propane and the subsequent formation of G-type or H-type phenyl propane as a consequence of ozone pretreatment. On the other hand, it can be attributed to the preferential degradation of S-type structural units by ozone molecules [35,36], resulting in a reduction in the S/G ratio of lignin from 3.1 (MWL) to 3.0 (OL60) and 2.7 (OL120). The S-type structural unit contains two methoxyl groups, and a decrease in the S/G ratio often signifies a decrease in the hydrophobic nature of the lignin [31]. Furthermore, p-CA is primarily linked to lignin or carbohydrates via ester bonds, while FA is bound to lignin through ether bonds and serves as a connecting agent between lignin and carbohydrates through ester bonds. The application of ozone pretreatment resulted in an augmentation of p-CA and FA levels within the MWL. Additionally, the augmentation of hydrophilic groups, such as coumarate and ferulate, is advantageous for reducing the hydrophobicity of lignin.

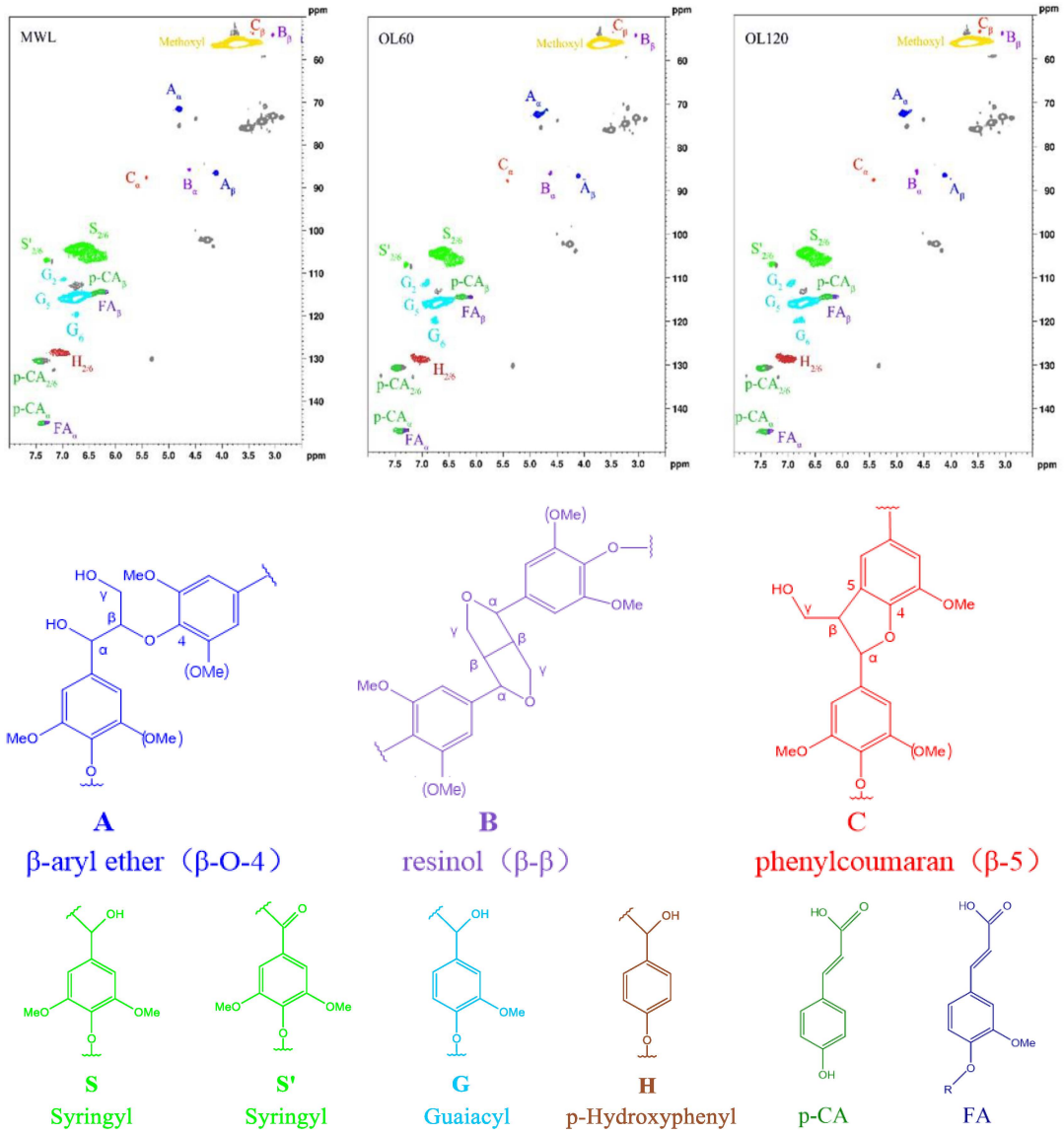

Figure 3. The HSQC-NMR spectrum of lignin before and after ozone pretreatment (A: Aryl ether bond; B: Resinol; C: Phenylcoumaran; S: Syringyl; S′: Oxidized syringyl; G: Guaiacyl; H: P-hydroxyphenyl; p-CA: P-coumarate; FA: Ferulate).

Table 3. Semi-quantification of lignin samples by HSQC-NMR.

Lignin Structure	Lignin Samples (%)		
	MWL	OL60	OL120
β-O-4 [1]	23.3	24.9	26.4
β-β [1]	5.8	6.6	8.0
β-5 [1]	4.5	5.1	6.5
S [2]	59.9	57.8	56.1
G [2]	18.8	19.7	21.1
H [2]	20.7	21.1	22.8
S/G [3]	3.2	3.0	2.7
p-CA	15.0	16.2	15.9
FA	1.5	1.9	1.8

Notes: [1] $I_x\% = \{I_x/[I\ (\beta\text{-O-4}) + I\ (\beta\text{-}\beta) + I\ (\beta\text{-5})]\} \times 100\%$; [2] $I_y\% = \{I_y/[I\ 0.5\ (S + S') + I\ (G) + I\ 0.5\ (H)]\} \times 100\%$; [3] $S/G = 0.5\ (S + S')/G$, where I_x and I_y represent the volume integrals of the lignin inter-unit connecting bonds and basic units to be measured, respectively [37,38].

3.4. Determination of Lignin Hydrophobicity by Rose Bengal

Hydrophobic interactions are considered to be the primary driving force behind the non-productive adsorption process of both lignin and cellulase. The hydrophobic properties of the lignin surface of ground wood were assessed using the Rose Bengal dye method to examine the alterations in hydrophobic interactions between lignin and cellulase prior to and following ozone pretreatment. It was found that ozone pretreatment resulted in a significant reduction in the hydrophobicity of MWL. Additionally, the surface hydrophobicity of OL 60 and OL 120 decreased from 0.951 L/g to 0.889 L/g and 0.615 L/g, respectively, representing a decrease of 6.5% and 35.3% (Table 4). This reduction can be attributed primarily to the ozone pretreatment, which induced the formation of hydrophilic groups such as carboxyl, carbonyl, p-coumarate, and ferulate, in lignin. Additionally, ozone's demethylation of methoxyl groups on the lignin benzene ring contributed to this reduction. These findings align with the characterization conducted using ^{31}P-NMR and HSQC-NMR techniques. Consequently, the decrease in the hydrophobic properties of the lignin surface led to a reduction in its binding affinity to cellulase, as reported by Wang et al. [39]. This subsequently minimized the ineffective adsorption of cellulase onto lignin [40].

Table 4. Hydrophobicity of lignin samples before and after ozone pretreatment.

Lignin	Lignin Samples		
	MWL	**OL60**	**OL120**
Hydrophobicity (L/g)	0.951	0.889	0.615

3.5. Determination of Zeta Potential

The role of electrostatic interaction is recognized as significant in the non-productive binding process between lignin and enzymes. As the pH of the solution employed in this experiment exceeded the isoelectric point (PI) of the cellulase utilized, the cellulase surface was negatively charged. The zeta potential of the lignin surface was examined in order to investigate the impact of ozone pretreatment on the charge properties of the lignin surface. The findings revealed that the negative zeta potential of MWL exhibited an increase following ozone pretreatment, with values of −11.8 mV and −15.5 mV for OL60 and OL120, respectively, representing a respective increase of 14.6% and 50.5% (Table 5). This increase can be attributed to the rise in the number of carboxyl groups and other groups in the lignin, resulting from ozone pretreatment [41]. Consequently, the electrostatic repulsion increased between ozone-pretreated MWL and cellulase, and effectively reduced the ineffective adsorption of cellulase onto lignin [42–44].

Table 5. Zeta potential of lignin samples before and after ozone pretreatment.

Lignin	Lignin Samples		
	MWL	**OL60**	**OL120**
zeta (mv)	−10.3	−11.8	−15.5

3.6. GPC Determination

In studying the macromolecular properties of lignin, gel permeation chromatography (GPC) is an important method. The average molecular weight (Mw), number average molecular weight (Mn), and polydispersity (PDI) of MWL were analysed by GPC. It was believed that Mw highlights the significance of the highest molecular weight fraction in determining the average molecular weight, whereas Mn emphasizes the influence of the largest number of fractions on the average molecular weight. Competitive reactions involving depolymerization and condensation commonly occur in lignin during pretreatment [45]. Following ozone pretreatment, both the Mw and PDI of MWL exhibited an increase, while Mn exhibited a decrease (Table 6). This can be attributed to the initial depolymerization

reaction of lignin during ozone pretreatment, resulting in the production of small molecular phenolic compounds and consequently augmenting the population of lignin with low molecular weight. However, certain small molecular phenolic substances undergo condensation reactions with lignin macromolecular chains, thereby further elevating the molecular weight of certain lignin with higher molecular weight. Consequently, this results in a marginal increase in the Mw of lignin, which aligns with the findings obtained from the HSQC-NMR analysis. Moreover, an increase in polydispersity may be beneficial in reducing the adsorption of cellulase onto lignin [46].

Table 6. Molecular weight of lignin samples before and after ozone pretreatment.

Lignin	Lignin Samples		
	MWL	OL60	OL120
M_w (g/mol)	8879	8959	9301
M_n (g/mol)	4125	4051	4064
PDI (M_w/M_n)	2.15	2.21	2.29

3.7. Langmuir Isothermal Adsorption Analysis

The effect of ozone pretreatment on the maximum adsorption, Langmuir constant, and binding strength between lignin and cellulase was determined by Langmuir adsorption isotherms. The adsorption capacity (Γ_{max}) and Langmuir constant (K) of OL 60 were observed to decrease by 51.18% and 8.95%, respectively, following ozone pretreatment. Similarly, the maximum adsorption capacity and Langmuir constant of OL120 were found to decrease by 60.85% and 27.06%, respectively (Table 7). This phenomenon can be attributed to the significant reduction in hydrophobicity of MWL after ozone pretreatment, which weakens the hydrophobic adsorption between cellulase and lignin. Moreover, the MWL surface has a high negative charge, which enhances the electrostatic repulsion between cellulase and lignin. Furthermore, the application of ozone pretreatment induces a conspicuous reduction in the phenolic hydroxyl content of MWL. Consequently, this reduction led to a decrease in the quantity of cellulase binding sites present on the surface of the MWL, ultimately diminishing their adsorption affinity [47] and resulting in a decline in the hydrogen bonds formed between cellulase and lignin. Ultimately, this cascade of events ultimately culminated in a substantial decrease in the maximum adsorption capacity (Γ_{max}). As a result of these two significant reductions (Γ_{max} and K), the binding strength (R) decreased from 357.14 mL/g to 158.73 mL/g for OL 60 and 102.04 mL/g for OL120, respectively. Consequently, it can be inferred that the structural alterations caused by ozone pretreatment lead to a decrease in non-productive binding interactions between lignin and cellulase.

Table 7. Langmuir-adsorption-isotherm parameters derived from cellulase adsorption on lignin.

Lignin Samples		Γ_{max} (mg/g)	K (mL/mg)	R (mL/g)	R^2
Lignin	MWL	25.77	13.86	357.14	0.980
	OL60	12.58	12.62	158.73	0.977
	OL120	10.09	10.11	102.04	0.958

4. Conclusions

In this work, the physical structure and chemical properties of ozone-pretreated MWL and its effect on the adsorption of cellulase were investigated. The ozone pretreatment has demonstrated efficacy and has been observed to induce alterations in the structure of lignin macromolecules, leading to an increase in the carboxyl content of lignin and a decrease in the S/G ratio, thereby weakening its hydrophobicity. Additionally, the oxidation process enhanced the negative charge on the MWL surface, leading to an increase in the electrostatic repulsion between lignin and cellulase. Consequently, the interaction between lignin and cellulase has been weakened, resulting in a decrease of over 60% in both the adsorption

capacity and binding strength of lignin to cellulase. This diminution resulted in a notable decrease in the inhibitory impact of lignin on cellulase hydrolysis, thereby overcoming the limitation imposed by the unproductive adsorption of lignin onto cellulase.

Author Contributions: C.Z.: Conceptualization, methodology, investigation, data curation, writing—original draft; L.Z.: supervision, writing—review and editing; W.L.: supervision; J.R.: supervision; H.W.: methodology, data curation; B.H.: supervision, writing—review, resources. All authors have read and agreed to the published version of the manuscript.

Funding: This work was supported by the National Natural Science Foundation of China (No. 22008079).

Institutional Review Board Statement: Not applicable.

Informed Consent Statement: Not applicable.

Data Availability Statement: Data are contained within the article.

Conflicts of Interest: The authors declare no conflicts of interest.

References

1. Chen, Z.; Chen, L.; Khoo, K.S.; Gupta, V.K.; Sharma, M.; Show, P.L.; Yap, P.S. Exploitation of lignocellulosic-based biomass biorefinery: A critical review of renewable bioresource, sustainability and economic views. *Biotechnol. Adv.* **2023**, *69*, 108265. [CrossRef] [PubMed]
2. Anastasovski, A. Improvement of Energy Efficiency in Ethanol Production Supported with Solar Thermal Energy—A Case Study. *Clean. Prod.* **2020**, *278*, 123476. [CrossRef]
3. Li, Y.; Bhagwat, S.S.; Cortés-Peña, Y.R.; Ki, D.; Rao, C.V.; Jin, Y.; Guest, J.S. Sustainable Lactic Acid Production from Lignocellulosic Biomass. *ACS Sustain. Chem. Eng.* **2021**, *9*, 1341–1351. [CrossRef]
4. Ibrahim, M.F.; Kim, S.W.; Abd-Aziz, S. Advanced bioprocessing strategies for biobutanol production from biomass. *Renew. Sustain. Energy Rev.* **2018**, *91*, 1192–1204. [CrossRef]
5. Tian, Y.; Zhang, F.; Wang, J.; Cao, L.; Han, Q. A review on solid acid catalysis for sustainable production of levulinic acid and levulinate esters from biomass derivatives. *Bioresour. Technol.* **2021**, *342*, 125977. [CrossRef]
6. Zhang, Y.; Xu, X.; Zhang, Y.; Li, J. Effect of adding surfactant for transforming lignocellulose into fermentable sugars during biocatalysing. *Biotechnol. Bioprocess Eng.* **2011**, *16*, 930–936. [CrossRef]
7. Sammond, D.W.; Yarbrough, J.M.; Mansfield, E.; Bomble, Y.J.; Hobdey, S.E.; Decker, S.R.; Taylor, L.E.; Resch, M.G.; Bozell, J.J.; Himmel, M.E. Predicting enzyme adsorption to lignin films by calculating enzyme surface hydrophobicity. *Biol. Chem.* **2014**, *289*, 20960–20969. [CrossRef]
8. Lou, H.; Zhu, J.Y.; Lan, T.Q.; Lai, H.; Qiu, X. pH-Induced lignin surface modification to reduce nonspecific cellulase binding and enhance enzymatic saccharification of lignocelluloses. *ChemSusChem* **2013**, *6*, 919–927. [CrossRef]
9. Nakagame, S.; Chandra, R.P.; Kadla, J.F.; Saddler, J.N. The isolation, characterization, and effect of lignin isolated from steam pretreated Douglas-fir on the enzymatic hydrolysis of cellulose. *Bioresour. Technol.* **2011**, *102*, 4507–4517. [CrossRef]
10. Yu, Z.; Gwak, K.S.; Treasure, T.; Jameel, H.; Chang, H.M.; Park, S. Effect of lignin chemistry on the enzymatic hydrolysis of woody biomass. *ChemSusChem* **2014**, *7*, 1942–1950. [CrossRef]
11. Pan, X. Role of functional groups in lignin inhibition of enzymatic hydrolysis of cellulose to glucose. *J. Biobased Mater. Bioenergy* **2008**, *2*, 25–32. [CrossRef]
12. Dias, M.O.S.; Da Cunha, M.P.; Maciel Filho, R.; Bonomi, A.; Jesus, C.D.F.; Rossell, C.E.V. Simulation of integrated first and second generation bioethanol production from sugarcane: Comparison between different biomass pretreatment methods. *J. Ind. Microbiol. Biotechnol.* **2011**, *38*, 955–966. [CrossRef] [PubMed]
13. Travaini, R.; Martín-Juárez, J.; Lorenzo-Hernando, A.; Bolado-Rodríguez, S. Ozonolysis: An advantageous pretreatment for lignocellulosic biomass revisited. *Bioresour. Technol.* **2016**, *199*, 2–12. [CrossRef]
14. Barrera-Martínez, I.; Guzmán, N.; Peña, E.; Vázquez, T.; Cerón-Camacho, R.; Folch, J.; Honorato Salazar, J.A.; Aburto, J. Ozonolysis of alkaline lignin and sugarcane bagasse: Structural changes and their effect on saccharification. *Biomass Bioenergy* **2016**, *94*, 167–172. [CrossRef]
15. Rosen, Y.; Mamane, H.; Gerchman, Y. Immersed ozonation of agro-wastes as an effective pretreatment method in bioethanol production. *Renew. Energy* **2021**, *174*, 382–390. [CrossRef]
16. Wang, H.; Zhao, L.; Ren, J.; He, B. Structural Changes of Alkali Lignin under Ozone Treatment and Effect of Ozone-Oxidized Alkali Lignin on Cellulose Digestibility. *Processes* **2022**, *10*, 559. [CrossRef]
17. Granata, A.; Argyropoulos, D. 2-Chloro-4,4,5,5-tetramethyl-1,3,2-dioxaphospholane, a Reagent for the Accurate Determination of the Uncondensed and Condensed Phenolic Moieties in Lignins. *J. Agric. Food Chem.* **1995**, *43*, 1538–1544. [CrossRef]
18. Li, X.; Li, M.; Pu, Y.; Ragauskas, A.J.; Klett, A.S.; Thies, M.; Zheng, Y. Inhibitory effects of lignin on enzymatic hydrolysis: The role of lignin chemistry and molecular weight. *Renew. Energy* **2018**, *123*, 664–674. [CrossRef]

19. Meng, X.; Crestini, C.; Ben, H.; Hao, N.; Pu, Y.; Ragauskas, A.; Argyropoulos, D. Determination of hydroxyl groups in biorefinery resources via quantitative ^{31}P NMR spectroscopy. *Nat. Protoc.* **2019**, *14*, 2627–2647. [CrossRef]
20. Li, G.; Ho, K.K.H.Y.; Zuo, Y.Y. Relative Dye Adsorption Method for Determining the Hydrophobicity of Nanoparticles. *J. Phys. Chem. C* **2022**, *126*, 832–837. [CrossRef]
21. Lange, H.; Rulli, F.; Crestini, C. Gel Permeation Chromatography in Determining Molecular Weights of Lignins: Critical Aspects Revisited for Improved Utility in the Development of Novel Materials. *ACS Sustain. Chem. Eng.* **2016**, *4*, 5167–5180. [CrossRef]
22. Yao, L.; Yang, H.; Yoo, C.G.; Chen, C.; Meng, X.; Dai, J.; Yang, C.; Yu, J.; Ragauskas, A.J.; Chen, X. A mechanistic study of cellulase adsorption onto lignin. *Green Chem.* **2021**, *23*, 333–339. [CrossRef]
23. Yang, H.; Yoo, C.G.; Meng, X.; Pu, Y.; Muchero, W.; Tuskan, G.A.; Tschaplinski, T.J.; Ragauskas, A.J.; Yao, L. Structural changes of lignins in natural *Populus* variants during different pretreatments. *Bioresour. Technol.* **2020**, *295*, 122240. [CrossRef] [PubMed]
24. Faix, O. Classification of lignins from different botanical origins by FT-IR spectroscopy. *Holzforschung* **1991**, *45*, 21–27. [CrossRef]
25. Guo, F.; Shi, W.; Sun, W.; Li, X.; Wang, F.; Zhao, J.; Qu, Y. Differences in the adsorption of enzymes onto lignins from diverse types of lignocellulosic biomass and the underlying mechanism. *Biotechnol. Biofuels* **2014**, *7*, 38. [CrossRef] [PubMed]
26. Wang, W.; Zhang, C.; Tong, S.; Cui, Z.; Liu, P. Enhanced enzymatic hydrolysis and structural features of corn stover by NaOH and ozone combined pretreatment. *Molecules* **2018**, *23*, 1300. [CrossRef] [PubMed]
27. Balakshin, M.; Capanema, E. On the quantification of lignin hydroxyl groups with ^{31}P and ^{13}C NMR spectroscopy. *J. Wood Chem. Technol.* **2015**, *35*, 220–237. [CrossRef]
28. Yao, L.; Xiong, L.; Yoo, C.G.; Dong, C.; Meng, X.; Dai, J.; Ragauskas, A.J.; Yang, C.; Yu, J.; Yang, H. Correlations of the physicochemical properties of organosolv lignins from *Broussonetia papyrifera* with their antioxidant activities. *Sustain. Energy Fuels* **2020**, *4*, 5114–5119. [CrossRef]
29. More, A.; Elder, T.; Pajer, N.; Argyropoulos, D.S.; Jiang, Z. Novel and Integrated Process for the Valorization of Kraft Lignin to Produce Lignin-Containing Vitrimers. *ACS Omega* **2023**, *8*, 1097–1108. [CrossRef]
30. Shi, C.; Zhang, S.; Wang, W.; Linhardt, R.J.; Ragauskas, A.J. Preparation of Highly Reactive Lignin by Ozone Oxidation: Application as Surfactants with Antioxidant and Anti-UV Properties. *ACS Sustain. Chem. Eng.* **2020**, *8*, 22–28. [CrossRef]
31. Wu, K.; Ying, W.; Shi, Z.; Yang, H.; Zheng, Z.; Zhang, J.; Yang, J. Fenton reaction-oxidized bamboo lignin surface and structural modification to reduce nonproductive cellulase binding and improve enzyme digestion of cellulose. *ACS Sustain. Chem. Eng.* **2018**, *6*, 3853–3861. [CrossRef]
32. Shi, Z.; Xiao, L.; Deng, J.; Xu, F.; Sun, R. Physicochemical characterization of lignin fractions sequentially isolated (*Dendrocalamus brandisii*) with hot water and alkaline ethanol solution. *J. Appl. Polym. Sci.* **2012**, *125*, 3290–3301. [CrossRef]
33. Wei, X.; Yu, Y.; Shen, Z.; Liu, Y.; Liu, X.; Wang, S.; Zhang, L.; Min, D. Deciphering the linkage type and structural characteristics of the *p*-hydroxyphenyl unit in *Pinus massoniana* Lamb compressed wood lignin. *Int. J. Biol. Macromol.* **2022**, *208*, 772–781. [CrossRef] [PubMed]
34. Domínguez-Robles, J.; Sánchez, R.; Espinosa, E.; Savy, D.; Mazzei, P.; Piccolo, A.; Rodríguez, A. Isolation and Characterization of *Gramineae* and *Fabaceae* Soda Lignins. *Int. J. Mol. Sci.* **2017**, *18*, 327. [CrossRef] [PubMed]
35. Figueirêdo, M.B.; Deuss, P.J.; Venderbosch, R.H.; Heeres, H.J. Valorization of Pyrolysis Liquids: Ozonation of the Pyrolytic Lignin Fraction and Model Components. *ACS Sustain. Chem. Eng.* **2019**, *7*, 4755–4765. [CrossRef]
36. Figueirêdo, M.B.; Keij, F.W.; Hommes, A.; Deuss, P.J.; Venderbosch, R.H.; Yue, J.; Heeres, H.J. Efficient Depolymerization of Lignin to Biobased Chemicals Using a Two-Step Approach Involving Ozonation in a Continuous Flow Microreactor Followed by Catalytic Hydrotreatment. *ACS Sustain. Chem. Eng.* **2019**, *7*, 18384–18394. [CrossRef]
37. Cheng, K.; Sorek, H.; Zimmermann, H.; Wemmer, D.E.; Pauly, M. Solution-state 2D NMR spectroscopy of plant cellwalls enabled by a dimethylsulfoxide-d 6/1-ethyl-3-methylimidazolium acetate solvent. *Anal. Chem.* **2013**, *85*, 3213–3221. [CrossRef]
38. Wen, J.; Sun, S.; Xue, B.; Sun, R. Recent advances in characterization of lignin polymer by solution-state nuclear magnetic resonance (NMR) methodology. *Materials* **2013**, *6*, 359–391. [CrossRef]
39. Wang, J.; Hao, X.; Wen, P.; Zhang, T.; Zhang, J. Adsorption and desorption of cellulase on/from lignin pretreated by dilute acid with different severities. *Ind. Crops Prod.* **2020**, *148*, 112309. [CrossRef]
40. Yang, Q.; Pan, X. Correlation between lignin physicochemical properties and inhibition to enzymatic hydrolysis of cellulose. *Biotechnol. Bioeng.* **2016**, *113*, 1213–1224. [CrossRef]
41. Wang, J.; Wang, J.; Lu, Z.; Zhang, J. Adsorption and desorption of cellulase on/from enzymatic residual lignin after alkali pretreatment. *Ind. Crops Prod.* **2020**, *155*, 112811. [CrossRef]
42. Fritz, C.; Ferrer, A.; Salas, C.; Jameel, H.; Rojas, O.J. Interactions between cellulolytic enzymes with native, autohydrolysis, and technical lignins and the effect of a polysorbate amphiphile in reducing nonproductive binding. *Biomacromolecules* **2015**, *16*, 3878–3888. [CrossRef] [PubMed]
43. He, J.; Huang, C.; Lai, C.; Huang, C.; Li, X.; Yong, Q. Elucidation of structure-inhibition relationship of monosaccharides derived pseudo-lignin in enzymatic hydrolysis. *Ind. Crops Prod.* **2018**, *113*, 368–375. [CrossRef]
44. Saini, J.K.; Patel, A.K.; Adsul, M.; Singhania, R.R. Cellulase adsorption on lignin: A roadblock for economic hydrolysis of biomass. *Renew. Energy* **2016**, *98*, 29–42. [CrossRef]
45. Yao, L.; Chen, C.; Yoo, C.G.; Meng, X.; Li, M.; Pu, Y.; Ragauskas, A.J.; Dong, C.; Yang, H. Insights of ethanol organosolv pretreatment on lignin properties of *Broussonetia papyrifera*. *ACS Sustain. Chem. Eng.* **2018**, *6*, 14767–14773. [CrossRef]

46. Berlin, A.; Balakshin, M.; Gilkes, N.; Kadla, J.; Maximenko, V.; Kubo, S.; Saddler, J. Inhibition of cellulase, xylanase and β-glucosidase activities by softwood lignin preparations. *J. Biotechnol.* **2006**, *125*, 198–209. [CrossRef]
47. Li, M.; Yi, L.; Bin, L.; Zhang, Q.; Song, J.; Jiang, H.; Chen, C.; Wang, S.; Min, D. Comparison of nonproductive adsorption of cellulase onto lignin isolated from pretreated lignocellulose. *Cellulose* **2020**, *27*, 7911–7927. [CrossRef]